HHS Public Access

Author manuscript

Leukemia. Author manuscript; available in PMC 2019 November 09.

Published in final edited form as:

Leukemia. 2019 November ; 33(11): 2685–2694. doi:10.1038/s41375-019-0467-z.

Development and preclinical validation of a novel covalent ubiquitin receptor Rpn13 degrader in multiple myeloma

Yan Song[#1], **Paul M. C. Park**[#2], **Lei Wu**[2], **Arghya Ray**[1], **Sarah Picaud**[3], **Deyao Li**[2], **Virangika K. Wimalasena**[2], **Ting Du**[1], **Panagis Filippakopoulos**[3], **Kenneth C. Anderson**[1], **Jun Qi**[2], **Dharminder Chauhan**[1]

[1]LeBow Institute for Myeloma Therapeutics and Jerome Lipper Myeloma Center, Department of Medical Oncology, Dana-Farber Cancer Institute, Harvard Medical School, Boston, MA, USA

[2]Department of Cancer Biology, Dana-Farber Cancer Institute, Department of Medicine, Harvard Medical School, Boston, MA, USA

[3]University of Oxford, Oxford, UK

[#] These authors contributed equally to this work.

Abstract

Proteasome inhibition is an effective treatment for multiple myeloma (MM); however, targeting different components of the ubiquitin–proteasome system (UPS) remains elusive. Our RNA-interference studies identified proteasome-associated ubiquitin-receptor Rpn13 as a mediator of MM cell growth and survival. Here, we developed the first degrader of Rpn13, WL40, using a small-molecule-induced targeted protein degradation strategy to selectively degrade this component of the UPS. WL40 was synthesized by linking the Rpn13 covalent inhibitor RA190 with the cereblon (CRBN) binding ligand thalidomide. We show that WL40 binds to both Rpn13 and CRBN and triggers degradation of cellular Rpn13, and is therefore first-in-class in exploiting a covalent inhibitor for the development of degraders. Biochemical and cellular studies show that WL40-induced Rpn13 degradation is both CRBN E3 ligase- and Rpn13-dependent. Importantly, WL40 decreases viability in MM cell lines and patient MM cells, even those resistant to bortezomib. Mechanistically, WL40 interrupts Rpn13 function and activates caspase apoptotic cascade, ER stress response and p53/p21 signaling. In animal model studies, WL40 inhibits

Kenneth C.Anderson Kenneth_Anderson@dfci.harvard.edu, Jun Qi Jun_Qi@dfci.harvard.edu, Dharminder Chauhan Dharminder_Chauhan@dfci.harvard.edu.

These authors jointly supervised this work: Kenneth C. Anderson, Jun Qi, and Dharminder Chauhan

Author contributions DC conceptualized the project, designed and supervised all the research, analyzed the data, and wrote the manuscript; YS performed the majority of experiments, generated CRSPR-Cas9 Rpn13-knockout cells, and analyzed the data; LW performed molecule synthesis of WL40; PMCP designed and performed AlphaScreen assays for the CRBN and RPN13 and analyzed the data; AR performed flow cytometry and SCID mouse studies; TD carried out western blotting; SP and PF purified RPN13 protein. VKW and DL reviewed the manuscript. JQ designed biochemical experiments and molecule, and reviewed the manuscript; KCA provided clinical samples, reviewed the data, and wrote the manuscript.

Supplementary information The online version of this article (https://doi.org/10.1038/s41375–019-0467-z) contains supplementary material, which is available to authorized users.

Compliance with ethical standards

Conflict of interest KCA is on Advisory board of Celgene, Millenium-Takeda, Gilead, Janssen, and Bristol Myers Squibb, and is a Scientific Founder of Oncopep and C4 Therapeutics. DC is consultant to Stemline Therapeutic, Inc., and Equity owner in C4 Therapeutics. All the remaining authors declare no conflict of interest.

xenografted human MM cell growth and prolongs survival. Overall, our data show the development of the first UbR Rpn13 degrader with potent anti-MM activity, and provide proof of principle for the development of degraders targeting components of the UPS for therapeutic application.

Introduction

Multiple myeloma (MM) accounts for 10% of all hemato-logic malignancies and affects 30,200 new individuals annually in the United States, highlighting the need for development of novel therapeutic approaches. Proteasome inhibitors (PIs), such as bortezomib, carfilzomib, and ixazomib are FDA-approved drugs used for the treatment of relapsed/refractory and newly diagnosed MM [1–4]. Although PI therapies have contributed to major advances, their clinical use has been associated with adverse effects and the emergence of drug resistance, underlying relapse of disease [2–5]. Importantly, the ability of PIs to overcome resistance to conventional therapies has validated the ubiquitin–proteasome system (UPS) as a therapeutic target in MM. Other than the 20S proteasome holoenzyme, which is targeted by PIs [6–9], there are several other potential therapeutic targets within the UPS including deubiquitinating enzymes or ubiquitin receptors (UbRs), which represent targets to enhance or even overcome PI resistance.

Our and other studies have focused on validating and targeting the UbR Rpn13/ADRM1 upstream of the 20S proteasome in cancers and in MM in particular [10–14]. Rpn13 is associated with the 19S regulatory component of the proteasome and plays a key role in directing ubiquitinated substrates for degradation via the 20S proteasome [15–17]. Specifically, Rpn13 captures the ubiquitinated proteins as substrate, followed by removal of ubiquitin moieties from the substrate by deubiquitinating enzymes UCH37 at the 19S proteasome; the target protein is then unfolded by the AAA-ATPases for 20S proteasome-mediated degradation. To date, strategies to delineate the functionality of Rpn13 used genetic modulation and small-molecule inhibitors [10, 12, 14, 18, 19]. For example, we showed that Rpn13 expression level is higher in MM cells than in normal plasma cells and that Rpn13 mediates MM cell growth and survival [10]; both RNA interference and a proof-of-concept Rpn13 inhibitor RA190 [11] confirmed that inhibiting Rpn13 induces MM cell growth inhibition [10]. Another study used a peptoid Rpn13 inhibitor to show antitumor responses [13]. However, currently there are no clinical grade agents targeting Rpn13.

Small-molecule inhibitors have shown clinical efficacy in many cancers, but their utility may be limited since (1) high systemic concentrations are required to inhibit disease-related target proteins to achieve clinical benefits, which triggers off-target binding activities; (2) inhibitors usually block the activity of one domain of multidomain proteins, leaving the functional properties of other domains intact. For example, Rpn13 inhibitor RA190 covalently reacts with cysteine residue 88 (Cys88) of Rpn13 Pru domain, but its interaction with the DEUBAD domain of Rpn13 is more labile due to the lack of a favorable binding pocket [11, 20, 21]; and (3) inhibition of target proteins may trigger compensatory feedback mechanisms including protein over-expression/accumulation, resulting in inadequate inhibition of the protein [22, 23]. Inspired by the recent strategy utilizing small molecules to

induce targeted protein degradation, we explored this alternative strategy by designing a small-molecule-based degrader to eliminate Rpn13 at the protein level. With both the inhibitor and degrader, we evaluated if protein degradation may overcome these limitations of small-molecule inhibitors.

Recent medicinal chemistry-based research led to the discovery of a mechanism-based chemical strategy for endogenous target protein degradation by using heterobifunctional small-molecule ligands to recruit E3 ubiquitin ligases to induce target protein degradation [22–28]. Degronimids, also known as proteolysis-targeting chimeras, are designed by conjugating the small-molecule binder of the target protein to an E3 ubiquitin ligase binding scaffold, such as the analogs of thalidomide for cereblon (CRBN) or ligands that bind to von Hippel–Lindau. Mechanistically, the degraders engage the target protein and recruit it to the E3 ubiquitin ligase, thereby promoting its ubiquitination and subsequent degradation by the proteasome [29]. This strategy has been applied to several proteins including the bromodomain and extra terminal family (BRD2, BRD3, and BRD4), BCR-ABL, FKBP12, ERRα, and RIPK2 [25, 29–31].

In the current study, we designed a small-molecule inducer of Rpn13 degradation, WL40, by linking the Rpn13 inhibitor, RA190, to an immunomodulatory drug (IMiD) (thalidomide) as a ligand for CRBN E3 ligase. WL40 promotes ligand-induced degradation of Rpn13 by the proteasome, which is the first of its kind to utilize a covalent inhibitor as the targeted protein binder. Using both in vitro and in vivo preclinical models and MM patient cells, we further confirmed that WL40 triggers potent anti-MM activity, overcoming PI resistance. Collectively, our results show the promising anti-MM activity of the first Rpn13 degrader, WL40, and provide the scaffold for the development of degraders targeting components of the UPS for therapeutic application.

Materials and methods

Chemical synthesis of WL40

Detailed synthesis and characterization of all compounds are provided in Supplemental Information. All the chemical reagents were purchased from Sigma-Aldrich with proper quality control. The compound WL40 is fully characterized using ^{1}HNMR, ^{13}CNMR, and MS, based on the American Chemical Society guidelines. RA190 and WL40 were synthesized in the Qi laboratory and were fully characterized using ^{1}HNMR, ^{13}CNMR, and MS, based on the American Chemical Society guidelines.

Biochemical assay conditions

The biochemical assays for both CRBN binding and RPN13 binding were performed with minimal modifications from the manufacturer’s protocol (PerkinElmer, USA). The assay details are described in Supplemental Information.

Cell culture and reagents

Human MM cell lines MM.1S, MM.1R, RPMI-8226, ANBL6.WT, ANBL6.BR, DOX40, INA6, and normal PBMCs were cultured in RPMI1640 complete medium. Informed consent

was obtained from all patients in accordance with the Helsinki protocol. MM CD138-positive cells, bone marrow stromal cells (BMSCs), and plasmacytoid dendritic cells (pDCs) from MM patients were isolated and cultured as described previously [32].

Immunoblotting

Cellular protein extracts were prepared using RIPA lysis buffer (50 mM Tris-HCl, 150 mM NaCl, 1% NP-40, 0.5% sodium deoxycholate, and 0.1% SDS). Protein lysates were subjected to immunoblotting using antibodies against poly ADP ribose polymerase (PARP, BD Bioscience Pharmingen, San Diego, CA), caspase-3, caspase-8, p53 (Santa Cruz Biotechnology), caspase-9, p-eIF2α (Abcam, Cambridge, MA), caspase-7, cyclin-B1, CDC25C, CDC2, p21, Rpn13, PERK, BIP, Calnexin, GFP, LC3A/B, α-tubulin (Cell Signaling, Beverly, MA), polyubiquitin (Enzo Life Sciences, Inc., Farmingdale, NY), or β-actin (Sigma-Aldrich, St. Louis, MO).

Proteasome activity assays

MM.1S cells were treated with WL40 (1 or 10 μM) or Bortezomib (1 μM) for 3 h; cells were then harvested and lysed in lysis buffer, followed by removal of debris by centrifugation. Total protein (25 μg) was analyzed for proteasome activity using the 20S proteasome Assay Kit (Calbiochem), as previously described [33].

Cell viability and apoptosis analysis

Cell viability was determined by WST-1/CellTiter-Glo Luminescent assays, as described previously [34]. Apoptosis was measured using Annexin/PI staining [33]. The caspase activity assay and cell cycle analysis were performed as described previously [35].

Generation of CRISPR/Cas9-knockout cell lines

We performed CRISPR/Cas9 genome editing to generate Rpn13-knockout (Rpn13-KO) HCT116 and MM.1S cell lines. Cells were transfected with Rpn13-CRISPR/Cas9-knockout (KO) plasmid (Santa Cruz Biotechnology, Inc., Santa Cruz, CA, USA) using Lipofectamine 2000 (Thermo Fisher Scientific, Waltham, MA, USA) or the cell line Nucleofector Kit V (Amaxa Biosystems, Cologne, Ger-many), respectively. After 48 h incubation, green fluorescent protein (GFP)-positive cells were sorted. Rpn13-KO was confirmed by both protein expression studies and DNA sequencing.

Human MM xenograft model

Animal model studies were performed as described previously [32, 33, 36]. Briefly, CB17 SCID mice were subcutaneously inoculated with 5.0×10^{6} MM. 1S cells. When tumors were measurable (100 mm^3) at ~3 weeks after MM-cell injection, mice (10 mice/group) were treated on a twice-weekly schedule with vehicle alone, WL40, or RA190. Mice were euthanized when tumor volume reached institutional limit (2000 mm^3). All animal experiment protocols were approved by and conformed to the relevant regulatory standards of the Institutional Animal Care and Use Committee at the Dana-Farber Cancer Institute.

Analysis of mice tumors

Tumors were harvested from WL40-treated and control animals. Tumor sections were fixed and paraffin-embedded for immunostaining to detect growth inhibition (Ki67), apoptosis (cleaved caspase-3), polyubiquitination (PolyU), and angiogenesis (CD31), as described previously [32, 34]. Tumor protein lysates from control vehicle- and WL40-treated mice were analyzed for caspase-8, poly-ubiquitin, or β-actin level using immunoblot analyses.

Statistical analysis

Statistical significance was derived using the two-tailed Student's *t*-test. Survival of mice was analyzed by Graph-Pad Prism software.

Results and discussion

Development of Rpn13 degrader

The main principle underlying the synthetic design of degraders is that bivalent molecules can interact with targeted proteins and E3 ligases simultaneously to induce the ubiquitination of targeted proteins. Therefore, we enlisted a small-molecule Rpn13 inhibitor, RA190, that covalently binds to Cys88 of the Rpn13 Pru domain. The covalent binding of RA190 to Rpn13 interrupts the recognition of polyubiquitinylated proteins that signals for subsequent degradation by the proteasome. Our degradation strategy utilized the E3 ligase, CRBN, and its binding molecules, IMiDs, one of which is thalidomide. These IMiDs bind to the E3 ubiquitin ligase complex (CUL4-RBX-DDB1 CRBN/$CRL4^{CRBN}$) and have also been used in the treatment of MM. More specifically, we linked RA190 with thalidomide via either an alkyl linker or a polyethylene glycol (PEG) linker to create a set of potential degraders. Amongst these compounds, WL40, created by linking RA190 to thalidomide with a short PEG linker, showed promising activity (Fig. 1a) as a potent degrader [37].

Specificity and functionality of WL40

We performed several experiments to confirm the specifi-city of WL40. Firstly, we assessed WL40-CRBN binding activity using in vitro AlphaScreen assays, as previously described [27]. Biochemical CRBN binding analysis confirmed that WL40 interacts with the E3 UbR CRBN using thalidomide and lenalidomide as positive controls (Fig. 1b). As expected, the Rpn13 inhibitor RA190 alone did not show any binding to CRBN (Fig. 1b). We then examined whether our bivalent molecule, WL40, can bind to Rpn13. We designed a novel biochemical AlphaScreen assay to measure compound binding to Rpn13 (Fig. 1c). Since Rpn13 recognizes polyubiquitin (polyUb), the GST-tagged Rpn13 and biotinylated polyUb are immobilized on the acceptor and donor beads of the AlphaScreen assay (obtained from PerkinElmer). Upon excitation, the donor bead releases a singlet of oxygen, which reaches the acceptor bead and creates an emission. The binding of RA190 and WL40 interrupts this recognition event and eliminates the signal. Using RA190 as a positive control, we further confirmed that WL40 binds to Rpn13 and interrupts Rpn13's recognition of the biotinylated polyubiquitin tail. (Fig. 1d). Thus, we confirmed that WL40 can bind both Rpn13 and CRBN complex.

We next examined whether WL40 decreases cellular Rpn13 levels in MM cells. MM.1S cells were treated with various concentrations of WL40 (200, 400, or 800 nM) for 4, 8, and 16 h; protein lysates were then analyzed for Rpn13 levels using immunoblot analysis. A marked decrease in Rpn13 levels was noted in WL40-treated cells in a time-dependent manner (Fig. 1e, upper panel). Decrease in Rpn13 levels was detectable as early as 8 h after WL40 treatment and maximally (95%) reduced at 16 h. Rpn13 protein level reduction was not observed with RA190 treatment (Fig. 1e, lower panel). There was no change in protein levels of tubulin, used as a loading control (Fig. 1e). To further corroborate our findings, we treated MM.1S cells with WL40, and then analyzed intracellular alterations in Rpn13 using flow cytometry. In concert with our data obtained using immunoblot analysis, a significant reduction in Rpn13 expression was noted in WL40- versus DMSO-, or RA190-treated cells (Fig. 1f).

To confirm that CRBN presence is a prerequisite for the function of WL40 in cells, we utilized CRBN-knockout (KO) MM.1S cells [27, 38], and examined the effect of WL40 on Rpn13 degradation. As shown in Fig. 1g, no decrease in Rpn13 levels was observed in WL40- versus DMSO control-treated CRBN-KO cells. These data demonstrate that WL40 degrades Rpn13 in a CRBN-dependent manner (Fig. 1g). We next utilized a Green Fluorescent Protein (GFP)u-1 reporter cell line expressing Ub-tagged GFP, which is marked for constitutive degra-dation by the proteasome. GFPu-1 cells were treated with WL40, and GFP levels were then analyzed using immunoblotting. As shown in Fig. 1h, WL40 treatment increases GFP levels, indicating the blockade of proteasomemediated GFP degradation. Similar results were observed in RA190-treated cells. These findings provide evidence for the requirement of Rpn13 engagement by WL40 for its activity (Fig. 1I). Thus, we have developed a novel degrader that can engage with both RPN13 and CRBN simulta-neously and induce targeted protein degradation.

To eliminate the potential impact of WL40 on protea-some function, we assessed the effect of WL40 on proteasome activities. Examination of both cellular extracts from WL40-treated MM cells and purified recombinant 20S proteasome showed that WL40 does not inhibit 20S proteasomal activities (chymotrypsin-like, trypsin-like, or caspase-like activities) (Fig. 2a, b). Pretreatment of MM.1S cells with the PI, MG132, blocked WL40-mediated Rpn13 degradation, suggesting that Rpn13 degradation occurs through the proteasome and that proteasome function is required for WL40-induced RPN13 degradation, consistent with other reports of targeted protein degradation (Fig. 2c). Together, these biochemical and cellular findings demonstrate that WL40 binds to CRBN and Rpn13 within cells and promotes ubiquitination of Rpn13, followed by subsequent proteasomal degradation of Rpn13.

We next evaluated the effect of WL40 on additional MM cell lines, including p53-mutated RPMI-8226 cells or bortezomib-resistant ANBL6.BR cells. WL40 (400 nM) treatment induced RPN13 degradation in both cell lines (Fig. 2d, e). We also examined whether WL40 triggers the accumulation of polyubiquitinated (PolyUb) protein, a hallmark event during proteasome inhibition, in these cell lines [39, 40] MM.1S and ANBL6.BR cells were treated with WL40, followed by analysis of ubiquitinated protein using immunoblotting. A marked increase in PolyUb proteins was detected in WL40- versus DMSO-treated cells (Fig. 2f).

PolyUb increase was also observed in bortezomib- and RA190-treated cells, albeit to a lesser extent than observed in WL40-exposed cells (Fig. 2f). The finding that WL40 triggered a more rapid and higher molecular weight PolyUb versus bortezomib suggests a distinct mechanism of action for these agents. Indeed, bortezomib only targets the 20S proteasomal activities and therefore leads to aggregation of lower molecular weight PolyUb proteins; whereas WL40 blocks the 19S proteasome and prevents deubiquitination of substrates, thereby resulting in higher molecular weight PolyUb proteins. Taken together, these data demonstrate that WL40 blocks proteasome-mediated protein degradation upstream of the 20S proteasome and promotes RPN13 degradation selectively, without inhibiting proteasomal activities.

Anti-MM activity of WL40

In order to examine whether WL40-triggerred Rpn13 degradation affects the viability of MM cells, we utilized a panel of MM cell lines sensitive or resistant to conventional (dexamethasone, alkylating agents, anthracyclines) or novel (bortezomib) therapies, including lines representing cytogenetically distinct MM subtypes. WL40 is more cytotoxic than the parental Rpn13 inhibitor RA190 against dexamethasone-sensitive MM.1S and resistant MM.1R isogenic MM cell lines (Fig. 3a), indicating potent anti-MM activity of WL40 versus RA190 due to its ability to degrade Rpn13. IC_{50} values for both MM.1S and MM.1R cells correlate with the DC_{50} for Rpn13. Importantly, WL40 overcomes bortezomib resistance, evidenced by similar IC_{50} values for both bortezomib-sensitive (ANBL6.WT) and -resistant (ANBL6.BR) cells (Fig. 3a, table). In addition, cytotoxic activity of WL40 was observed even against p53-mutated RPMI-8226 cells and MM growth factor IL-6-dependent INA6 MM cells (Fig. 3a, table). These data suggest that WL40 can overcome p53 mutation, a high-risk feature conferring drug resistance in MM, and triggers MM cell death even in the presence of pro-growth and -survival factor IL-6.

To further evaluate the clinical potential of our novel degrader, we next examined the effect of WL40 in MM patient cells. We first analyzed primary tumor ($CD138^+$) cells from newly diagnosed (patient #1) and MM refractory to bortezomib/lenalidomide (patients #2–4) (Fig. 3b). Treatment with WL40 decreased viability of all $CD138^+$ patient cells (IC_{50} range: 95–170 nM) (Fig. 3b). Impor-tantly, WL40 at the IC_{50} for MM cells does not affect viability of normal PBMCs (Fig. 3c), suggesting a favorable therapeutic index.

Adhesion of MM cells to BMSCs induces MM-promoting growth factors and protects against cytotoxic activity of anti-MM drugs [41, 42]. Moreover, BM accessory cells such as pDCs, can also trigger MM cell pro-liferation, survival, and drug resistance [32]. Therefore, we next assessed the effect of WL40 using our patient MM-BMSCs or MM-pDCs in vitro coculture assays. Even in these cocultures with BMSCs or pDCs, WL40 induced a dose-dependent decrease in the viability of MM cells. (Fig. 3d, e). These data demonstrate that WL40 retains its anti-MM activity in the tumor-protective MM-host BM microenvironment.

Rpn13 degradation-induced signal transduction

We next examined the downstream signaling triggered by WL40 during Rpn13 degradation. WL40 treatment induces an increase in early- (Annexin V^+/PI^-) and late-stage (Annexin V

$^{+}$/PI^{+}) apoptosis, associated with proteolytic cleavage of Poly (ADP) ribose polymerase (PARP) by immunoblotting, as well as activation of caspase-3, caspase-7, caspase-8 and caspase-9, assessed in caspase enzymatic activity assays (Fig. 4a–c, respectively). Additionally, treatment of MM.1S and ANBL6.BR cells with WL40 triggers a reduction in the levels of cell cycle regulatory proteins (cyclin-B1, CDC25C, and CDC2), indicating growth arrest in these cells (Fig. 4d). Examination of the p53/p21 apoptotic signaling axis showed an earlier induction of this pathway in WL40- versus Rpn13 inhibitor RA190-treated ANBL6.BR cells (Fig. 4e).

Elevated endoplasmic reticulum (ER)-associated protein degradation (ERAD) signaling is a hallmark of MM, which confers enhanced sensitivity to PIs. Since WL40, like botezomib, triggers PolyUb accumulation (Fig. 2f), we next examined whether it increases ER stress and triggers associated unfolded protein response (UPR) signaling. Indeed, we found a rapid and robust induction of UPR proteins (BIP, PERK, phosphorylated eIF2α, or a lectin protein calnexin) in WL40-treated ANBL6.BR and MM.1S cells (Fig. 4e, f, respectively). Of note, Rpn13 inhibitor RA190 also triggered UPR signaling, but with delayed kinetics and to a lesser extent than Rpn13 degrader WL40. Prior studies have established that ER stress also induces an alternative lysosomal pathway (autophagy) for degradation of misfolded proteins [40]. Here, we found that WL40 induces PERK, a key component in autophagic signaling. To further confirm the activation of autophagy by WL40, we examined alterations in the autophagic molecule LC3/Atg8. During autophagy, LC3/Atg8 is processed and attached to the autophagosome membrane by conjugation with phosphati-dylethanolamine. Immunoblot analysis showed a significant increase in LC3A/B in WL40- versus DMSO-treated ANBL6.BR or MM.1S cells (Fig. 4e, f, respectively). As for UPR signaling in ANBL6.BR cells, a more pronounced LC3 activation was noted after WL40 than RA190 treatment. Overall, these findings show that WL40-induced apoptosis is associated with activation of the caspase-cascade, p53/p21 signaling, ER stress response signaling, and autophagy. Importantly, we show that degradation of Rpn13 triggers more pronounced biologic sequelae in MM cells than domain-specific Rpn13 inhibition.

In vivo anti-MM activity of WL40

To fully understand the therapeutic potential of the RPN13 degrader, we evaluated the in vivo efficacy of WL40 using our human plasmacytoma xenograft mouse model [3, 34]. This model has been useful in validating novel anti-MM therapies bortezomib, carfilzomib, ixazomib, lenalidomide, and pomalidomide, which have translated to clinical trials and FDA approval. Treatment of MM.1S-bearing mice with intraperitoneal (IP) injections of WL40 (14.7 μM/kg) inhibits MM growth and prolongs host survival (Fig. 5a). Rpn13 inhibitor RA190 (26.8 μM/kg) also attenuates MM tumor progression and extends mice survival (Fig. 5a, b, respectively). Importantly, use of even half the equimolar dose of WL40 versus RA190 achieves similar extent of tumor growth inhibition and host survival. These findings suggest that Rpn13 degradation could be a more potent strategy in blocking tumor progression than Rpn13 inhibition. WL40 was well tolerated, with no significant weight loss in WL40-treated mice (data not shown). Analysis of tumors harvested from treated mice showed that WL40 induced increased accumulation of PolyUb proteins relative to tumors from control mice (Fig. 5c, d). WL40 decreases proliferation, induces apoptosis, and blocks

angiogenesis in harvested tumors, as assessed by Ki67, cleaved caspase-3, and CD31 staining, respectively (Fig. 5d). These data therefore show more potent in vivo anti-MM activity of WL40 versus RA190.

In summary, we here describe the development of a small-molecule degrader, WL40, targeting UbR Rpn13, and validate its specificity and functionality using both biochemical and genetic models. Importantly, our studies using both in vitro and in vivo preclinical models of MM show potent anti-MM activity of WL40. Novel findings include the following: (1) we demonstrate the development of the first covalent inhibitor-based heterobifunctional degrader molecule of Rpn13; (2) using both pharmacological assays and in vivo tumor efficacy models, we show that the Rpn13 degrader is cell permeable and triggers potent anti-MM activity, even in the presence of cytoprotective tumor BM microenvironment, overcomes bortezomib resistance, and is active even in the context of mutated-p53; (3) Rpn13 degradation is a more efficient inducer of MM cell death than Rpn13 inhibition, evidenced by a more rapid and robust induction of ER stress response/UPR- and p53/p21-apoptotic signaling by WL40 than RA190; (4) our MM xenograft model study showed that significant tumor growth inhibition can be achieved using half the equimolar dose of WL40 versus Rpn13 inhibitor RA190; and (5) our study strongly suggests that degradation of tumorpromoting proteins within the UPS using the degronimid strategy is a plausible therapeutic approach, especially in cancers with elevated ER stress/UPR signaling such as MM.

Finally, the anti-MM activity of the IMiD, lenalidomide, occurs via CRBN complex-mediated degradation of Ikaros proteins, IKZF1, and IKZF3 [38]. This finding supports the therapeutic potential of strategies to induce degradation of tumorigenic target proteins via chemically synthesized small-molecule degraders. Importantly, extensive preclinical research shows that degraders may: reduce the need to maintain high systemic inhibitor levels for target inhibition and efficacy in vivo; neutralize even high levels of target protein expression and function; as well as degrade substrates and thereby avoid resistance mechanisms such as gene mutation or copy number alterations. Overall, our present study provides the rationale for the development of UPS-based degrader therapies, and further indicates the potential clinical utility of novel therapeutics targeting UbR Rpn13 to improve patient outcome in MM.

Acknowledgments

The grant support for this investigation was provided by the National Institutes of Health Specialized Programs of Research Excellence (SPORE) grants P50100707, R01CA207237, and RO1CA050947. KCA is an American Cancer Society Clinical Research Professor.

References

1. Kane RC, Bross PF, Farrell AT, Pazdur R. Velcade: U.S. FDA approval for the treatment of multiple myeloma progressing on prior therapy. Oncologist 2003;8:508–13. [PubMed: 14657528]
2. Richardson PG, Barlogie B, Berenson J, Singhal S, Jagannath S, Irwin D, et al. A phase 2 study of bortezomib in relapsed, refractory myeloma. N Engl J Med 2003;348:2609–17. [PubMed: 12826635]

3. Anderson KC. Therapeutic advances in relapsed or refractory multiple myeloma. J Natl Compr Cancer Netw 2013;11(5 Suppl):676–9.
4. Richardson PG, Zweegman S, O'Donnell EK, Laubach JP, Raje N, Voorhees P, et al. Ixazomib for the treatment of multiple myeloma. Expert Opin Pharmacother 2018;19:1949–68. [PubMed: 30422008]
5. Lonial S, Waller EK, Richardson PG, Jagannath S, Orlowski RZ, Giver CR, et al. Risk factors and kinetics of thrombocytopenia associated with bortezomib for relapsed, refractory multiple myeloma. Blood 2005;106:3777–84. [PubMed: 16099887]
6. Adams J The proteasome: a suitable antineoplastic target. Nat Rev Cancer 2004;4:349–60. [PubMed: 15122206]
7. Goldberg AL. Protein degradation and protection against mis-folded or damaged proteins. Nature 2003;426:895–9. [PubMed: 14685250]
8. Hershko A The ubiquitin system for protein degradation and some of its roles in the control of the cell division cycle. Cell Death Differ 2005;12:1191–7. [PubMed: 16094395]
9. Chauhan D, Hideshima T, Anderson KC. Proteasome inhibition in multiple myeloma: therapeutic implication. Annu Rev Pharmacol Toxicol 2005;45:465–76. [PubMed: 15822185]
10. Song Y, Ray A, Li S, Das DS, Tai YT, Carrasco RD, et al. Targeting proteasome ubiquitin receptor Rpn13 in multiple mye-loma. Leukemia 2016;30:1877–86. [PubMed: 27118409]
11. Anchoori RK, Karanam B, Peng S, Wang JW, Jiang R, Tanno T, et al. A bis-benzylidine piperidone targeting proteasome ubiquitin receptor RPN13/ADRM1 as a therapy for cancer. Cancer Cell 2013;24:791–805. [PubMed: 24332045]
12. Chen W, Hu XT, Shi QL, Zhang FB, He C. Knockdown of the novel proteasome subunit Adrm1 located on the 20q13 amplicon inhibits colorectal cancer cell migration, survival and tumor-igenicity. Oncol Rep 2009;21:531–7. [PubMed: 19148532]
13. Trader DJ, Simanski S, Kodadek T. A reversible and highly selective inhibitor of the proteasomal ubiquitin receptor rpn13 is toxic to multiple myeloma cells. J Am Chem Soc 2015;137: 6312–9. [PubMed: 25914958]
14. Fejzo MS, Dering J, Ginther C, Anderson L, Ramos L, Walsh C, et al. Comprehensive analysis of 20q13 genes in ovarian cancer identifies ADRM1 as amplification target. Genes Chromosomes Cancer 2008;47:873–83. [PubMed: 18615678]
15. Husnjak K, Dikic I. Ubiquitin-binding proteins: decoders of ubiquitin-mediated cellular functions. Annu Rev Biochem 2012; 81:291–322. [PubMed: 22482907]
16. Schreiner P, Chen X, Husnjak K, Randles L, Zhang N, Elsasser S, et al. Ubiquitin docking at the proteasome through a novel pleckstrin-homology domain interaction. Nature 2008;453:548–52. [PubMed: 18497827]
17. Lu X, Nowicka U, Sridharan V, Liu F, Randles L, Hymel D, et al. Structure of the Rpn13-Rpn2 complex provides insights for Rpn13 and Uch37 as anticancer targets. Nat Commun 2017;8:15540. [PubMed: 28598414]
18. Fejzo MS, Anderson L, Chen HW, Anghel A, Zhuo J, Anchoori R, et al. ADRM1-amplified metastasis gene in gastric cancer. Genes Chromosomes Cancer 2015;54:506–15. [PubMed: 26052681]
19. Carvalho B, Postma C, Mongera S, Hopmans E, Diskin S, van de Wiel MA, et al. Multiple putative oncogenes at the chromosome 20q amplicon contribute to colorectal adenoma to carcinoma progression. Gut 2009;58:79–89. [PubMed: 18829976]
20. Chen X, Walters KJ. Structural plasticity allows UCH37 to be primed by RPN13 or locked down by INO80G. Mol Cell 2015; 57:767–8. [PubMed: 25747657]
21. Anchoori RK, Jiang R, Peng S, Soong RS, Algethami A, Rudek MA, et al. Covalent Rpn13-binding inhibitors for the treatment of ovarian cancer. ACS Omega 2018;3:11917–29. [PubMed: 30288466]
22. Cromm PM, Crews CM. Targeted protein degradation: from chemical biology to drug discovery. Cell Chem Biol 2017;24: 1181–90. [PubMed: 28648379]
23. Burslem GM, Smith BE, Lai AC, Jaime-Figueroa S, McQuaid DC, Bondeson DP, et al. The advantages of targeted protein degradation over inhibition: an RTK case study. Cell Chem Biol 2018;25:67–77.e3. [PubMed: 29129716]

24. Gustafson JL, Neklesa TK, Cox CS, Roth AG, Buckley DL, Tae HS, et al. Small-molecule-mediated degradation of the androgen receptor through hydrophobic tagging. Angew Chem 2015;54: 9659–62. [PubMed: 26083457]
25. Lu J, Qian Y, Altieri M, Dong H, Wang J, Raina K, et al. Hijacking the E3 ubiquitin ligase cereblon to efficiently target BRD4. Chem Biol 2015;22:755–63. [PubMed: 26051217]
26. Sakamoto KM, Kim KB, Kumagai A, Mercurio F, Crews CM, Deshaies RJ. Protacs: chimeric molecules that target proteins to the Skp1-Cullin-F box complex for ubiquitination and degradation. Proc Natl Acad Sci USA 2001;98:8554–9. [PubMed: 11438690]
27. Winter GE, Buckley DL, Paulk J, Roberts JM, Souza A, Dhe-Paganon S, et al. DRUG DEVELOPMENT. Phthalimide conjugation as a strategy for in vivo target protein degradation. Science 2015;348:1376–81. [PubMed: 25999370]
28. Fischer ES, Park E, Eck MJ, Thoma NH. SPLINTS: small-molecule protein ligand interface stabilizers. Curr Opin Struct Biol 2016;37:115–22. [PubMed: 26829757]
29. Raina K, Crews CM. Targeted protein knockdown using small molecule degraders. Curr Opin Chem Biol 2017;39:46–53. [PubMed: 28605671]
30. Toure M, Crews CM. Small-molecule PROTACS: new approa-ches to protein degradation. Angew Chem 2016;55:1966–73. [PubMed: 26756721]
31. Nowak RP, DeAngelo SL, Buckley D, He Z, Donovan KA, An J. et al. Plasticity in binding confers selectivity in ligand-induced protein degradation. Nat Chem Biol 2018;14:706–14. [PubMed: 29892083]
32. Chauhan D, Singh AV, Brahmandam M, Carrasco R, Bandi M, Hideshima T, et al. Functional interaction of plasmacytoid den-dritic cells with multiple myeloma cells: a therapeutic target. Cancer Cell 2009;16:309–23. [PubMed: 19800576]
33. Chauhan D, Catley L, Li G, Podar K, Hideshima T, Velankar M, et al. A novel orally active proteasome inhibitor induces apoptosis in multiple myeloma cells with mechanisms distinct from borte-zomib. Cancer Cell 2005;8:407–19. [PubMed: 16286248]
34. Chauhan D, Tian Z, Nicholson B, Kumar KG, Zhou B, Carrasco R, et al. A small molecule inhibitor of ubiquitin-specific protease-7 induces apoptosis in multiple myeloma cells and overcomes bortezomib resistance. Cancer Cell 2012;22:345–58. [PubMed: 22975377]
35. Chauhan D, Ray A, Viktorsson K, Spira J, Paba-Prada C, Munshi N, et al. In vitro and in vivo antitumor activity of a novel alky-lating agent, melphalan-flufenamide, against multiple myeloma cells. Clin Cancer Res 2013;19:3019–31. [PubMed: 23584492]
36. Tian Z, Zhao JJ, Tai YT, Amin SB, Hu Y, Berger AJ, et al. Investigational agent MLN9708/2238 targets tumor-suppressor miR33b in MM cells. Blood 2012;120:3958–67. [PubMed: 22983447]
37. Ito T, Ando H, Suzuki T, Ogura T, Hotta K, Imamura Y, et al. Identification of a primary target of thalidomide teratogenicity. Science 2010;327:1345–50. [PubMed: 20223979]
38. Lu G, Middleton RE, Sun H, Naniong M, Ott CJ, Mitsiades CS, et al. The myeloma drug lenalidomide promotes the cereblon-dependent destruction of Ikaros proteins. Science 2014;343: 305–9. [PubMed: 24292623]
39. Menendez-Benito V, Verhoef LG, Masucci MG, Dantuma NP. Endoplasmic reticulum stress compromises the ubiquitin-proteasome system. Hum Mol Genet 2005;14:2787–99. [PubMed: 16103128]
40. Bravo R, Parra V, Gatica D, Rodriguez AE, Torrealba N, Paredes F, et al. Endoplasmic reticulum and the unfolded protein response: dynamics and metabolic integration. Int Rev Cell Mol Biol 2013;301:215–90. [PubMed: 23317820]
41. Chauhan D, Hideshima T, Mitsiades C, Richardson P, Anderson KC. Proteasome inhibitor therapy in multiple myeloma. Mol Cancer Ther 2005;4:686–92. [PubMed: 15827343]
42. Chauhan D, Uchiyama H, Akbarali Y, Urashima M, Yamamoto K, Libermann TA, et al. Multiple myeloma cell adhesion-induced interleukin-6 expression in bone marrow stromal cells involves activation of NF-kappa B. Blood 1996;87:1104–12. [PubMed: 8562936]

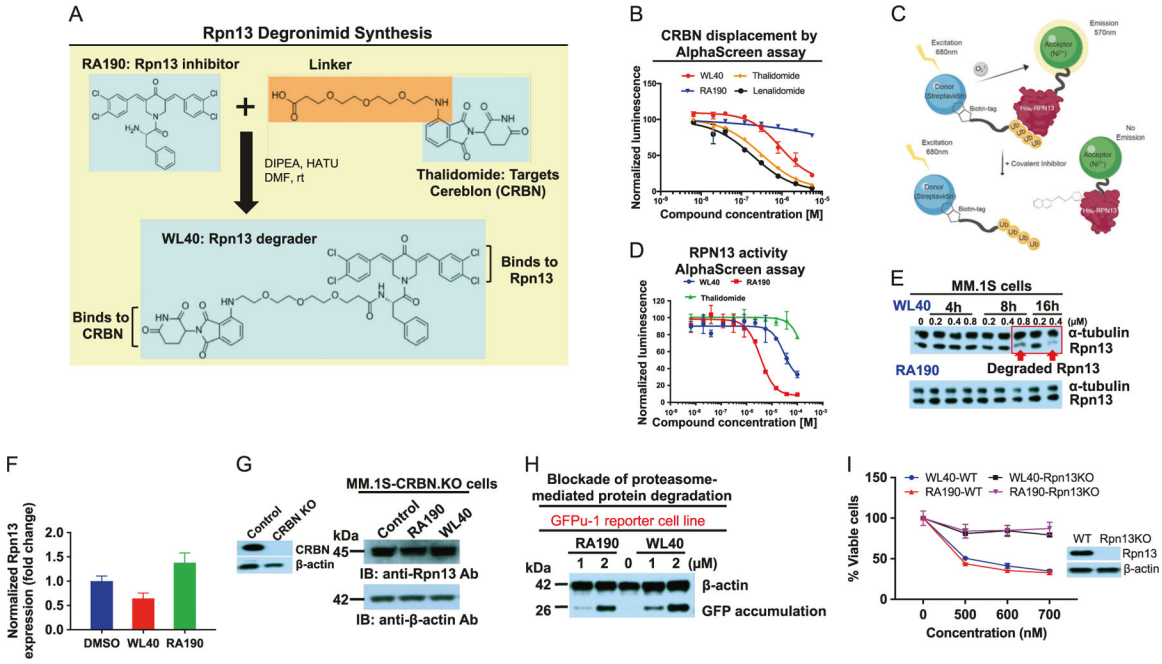

Fig. 1.

Design and characterization of Rpn13 degrader WL40. **a** WL40 was created by linking the Rpn13 inhibitor RA190 to the IMiD thalidomide as a ligand for the CRBN E3 ligase via a PEG linker. **b** The cereblon AlphaScreen assay to measure the displacement of biotinylated-pomalidomide probe (triplicate means ± SD). **c** Schematic cartoon for the novel AlphaScreen assay to measure the binding activity of inhibitor with RPN13 proteins. **d** The RPN13 AlphaScreen assay to measure the binding activity of inhibitor with RPN13 proteins (triplicate means ± SD). **e** MM.1S cells were treated with WL40 or RA190 at the indicated concentrations and time periods; protein lysates were subjected to immunoblot analysis using anti-Rpn13 or anti-tubulin Abs. **f** MM.1S cells were treated with DMSO control, WL40 (400 nM), or RA190 (500 nM) for 16 h; cells were then washed and stained with Rpn13 Ab conjugated with Alexa Fluor 647, followed by flow cytometry analysis. Isotype Ab conjugated to Alexa Fluor 647 was used as control for nonspecific binding. Data were quantified using FACS Diva (BD Biosciences, USA) and FlowJo (FlowJo LLC, USA). **g** MM.1S-CRBN-KO cells were treated with WL40 (400 nM) or RA190 (500 nM) for 16 h; protein lysates were subjected to immunoblot analysis using anti-Rpn13 or anti-β-actin Abs. Inset: protein lysates from MM.1S. WT control and MM.1S-CRBN-KO cells were subjected to immunoblot analysis using anti-CRBN or anti-β-actin Abs. **h** Immunoblot showing the levels of Ub-GFP accumulation in a GFPu-1 reporter cell line treated with indicated concentrations of WL40 and RA190 for 16 h. Blots shown are representative of three independent experiments. **i** HCT116-WT and HCT116-CRISPR Rpn13-KO cells were treated with WL40 or RA190 at the indicated concentrations for 48 h, followed by assessment of cell viability using the WST assay (mean ± SD; $p < 0.001$; $n = 3$). Inset: protein lysates from Rpn13-WT and KO cells were subjected to immunoblot analysis using anti-Rpn13 or β-actin Abs

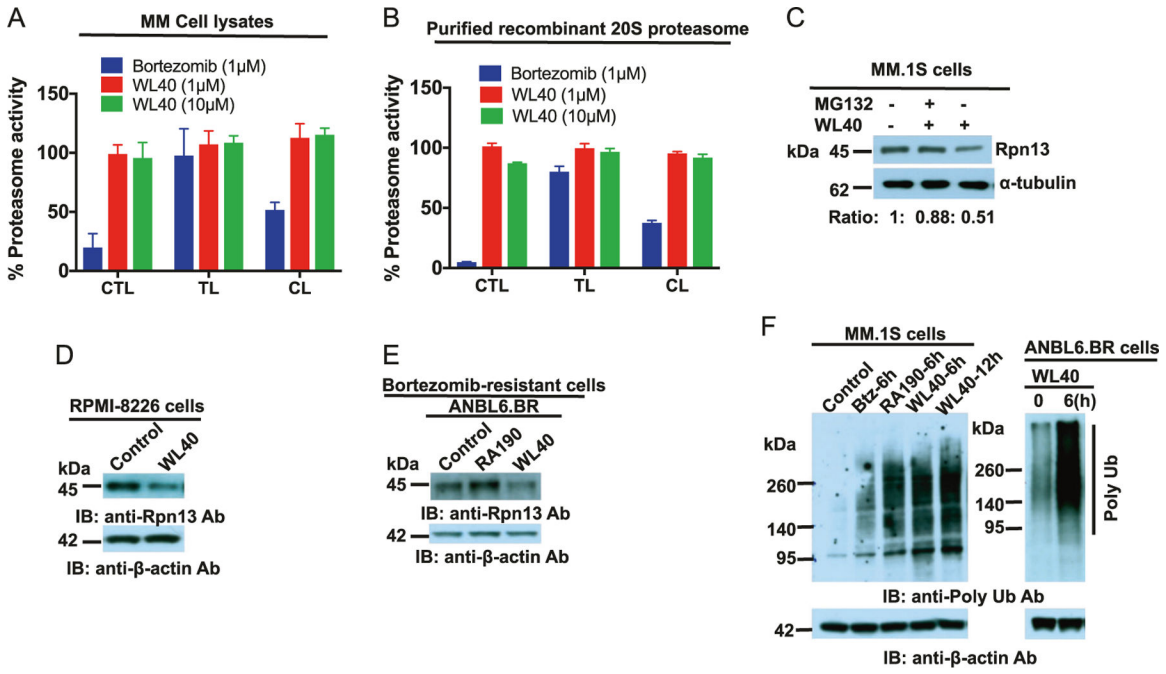

Fig. 2.

WL40 blocks proteasome-mediated protein degradation without inhibiting proteasome proteolytic activities. **a** MM.1S cells were treated with DMSO control, bortezomib, or WL40 at indicated concentration for 3 h; protein lysates were analyzed for proteasome activities (CT-L, chymotrypsin-like; T-L, trypsin-like; C-L, caspase-like). The percentage of proteasome activity was normalized to DMSO control (mean ± SD; $n = 3$). **b** Recombinant 20S proteasome was incubated with DMSO, bortezomib, or WL40 for 30 min, followed by assessment of proteasome activities. Bar graph shows percent pro-teasome activity after normalization with DMSO control (mean ± SD; $n = 3$). **c** MM.1S cells were pretreated with MG132 (10 μM) for 1 h, followed by addition of WL40 (400 nM) for 8 h. As a positive control for WL40-induced Rpn13 degradation, cells were also treated with WL40 alone for 8 h. Total protein lysates were subjected to immunoblots for Rpn13 and α-tubulin. **d** RPMI-8226 cells were treated with WL40 (400 nM) for 16 h; protein lysates were subjected to immuno-blot analysis using anti-Rpn13 or anti-β-actin Abs. **e** ANBL6.BR cells were treated with WL40 (400 nM) or RA190 (500 nM) for 16 h; protein lysates were subjected to immunoblot analysis using anti-Rpn13 or anti-β-actin Abs. **f** (Left panel) MM.1S cells were treated with DMSO control, bortezomib (5 nM), RA190 (300 nM), or WL40 (200 nM) for indicated time periods; protein lysates were subjected to immunoblot analysis using antipolyubiquitin or anti-β-actin Abs. f (Right panel) ANBL6.BR cells were treated with DMSO control or WL40 (1 μM) for 6 h; protein lysates were subjected to immunoblot analysis using antipolyubiquitin or anti-β-actin Abs

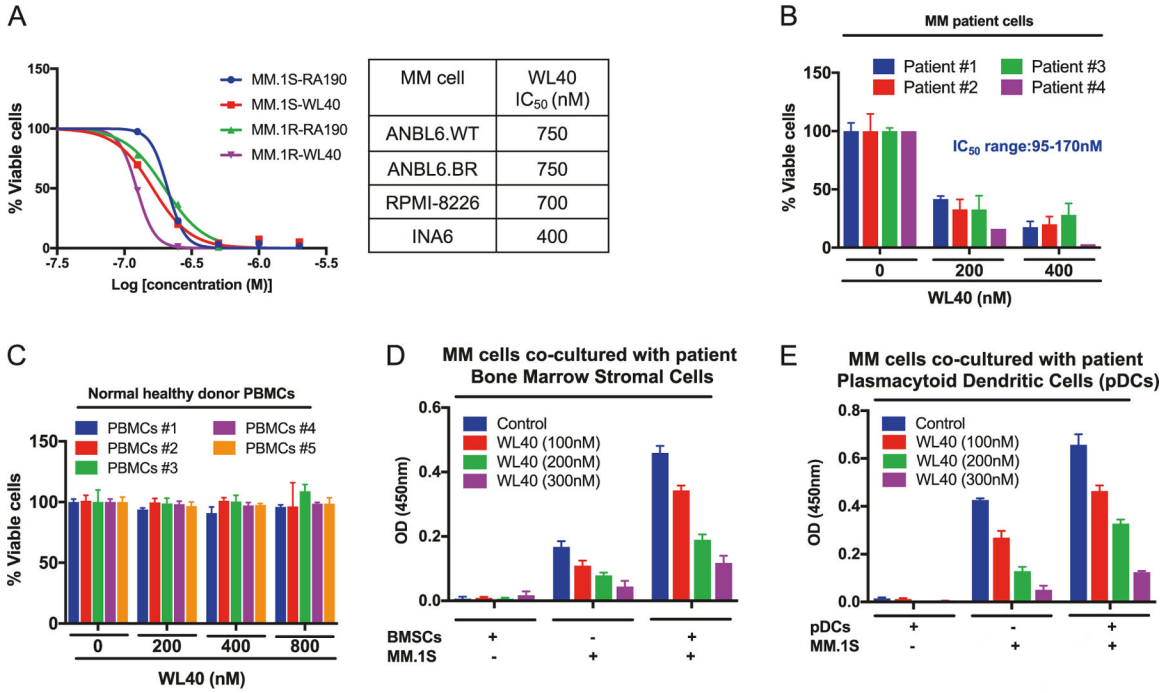

MM cell	WL40 IC_{50} (nM)
ANBL6.WT	750
ANBL6.BR	750
RPMI-8226	700
INA6	400

Fig. 3.

WL40 triggers anti-MM activity as well as overcomes bortezomib-resistance and cytoprotective activity of MM BM micro-environment. **a** MM.1S and MM.1R cells were treated with DMSO control, WL40, or RA190 at indicated concentrations for 48 h, followed by assessment for cell viability using the WST assay ($p < 0.05$ for both cell lines; $n = 3$). Table: ANBL6.WT, ANBL6.BR, RPMI-8226, or INA6 MM cell lines were treated with DMSO control of WL40 for 48 h, followed by assessment for cell viability. The IC_{50} of WL40 for cell lines is shown. **b** Purified $CD138^+$ patient MM cells were treated with DMSO control or WL40 at indicated concentrations for 48 h, followed by assessment for cell viability using the CellTiter-Glo assay (mean ± SD of triplicate cultures; $p < 0.001$). **c** Normal PBMCs from healthy donors were treated with DMSO control or WL40 at indicated concentrations for 48 h, and then analyzed for cell viability using the CellTiter-Glo assay (mean ± SD of quadruplicate cultures). **d** MM.1S cells were cultured with or without patient BMSCs in the presence or absence of WL40 for 48 h, and cell proliferation was measured by the WST assay (mean ± SD; $n = 3$; $p < 0.0001$). e MM.1S cells were cultured with or without patient plasmacytoid dendritic cells (pDCs) in the presence or absence of WL40 for 48 h, and cell pro-liferation was measured by the WST assay (mean ± SD; $n = 3$; $p <$ 0.0001)

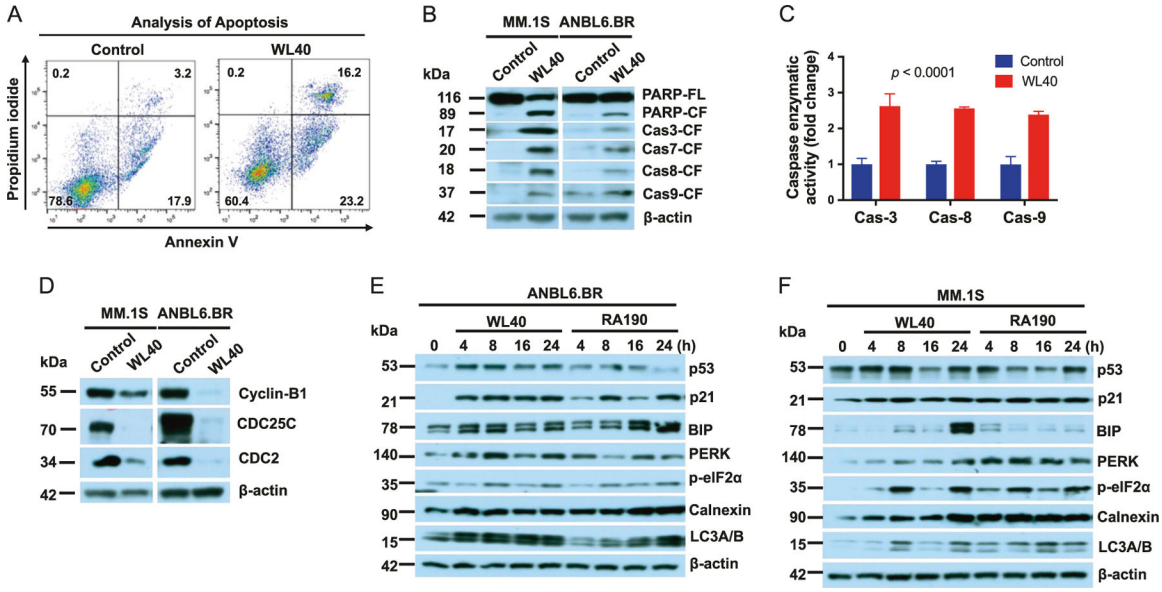

Fig. 4.

Mechanisms of WL40-induced MM cell death. **a** MM.1S cells were treated with DMSO control or WL40 (200 nM) for 16 h, and then analyzed for apoptosis using the Annexin V/PI double-staining assay (mean ± SD; $n = 3$; $p < 0.001$). **b** MM.1S and ANBL6.BR cells were treated with DMSO control or WL40 (200 nM for MM.1S; 1 μM for ANBL6.BR) for 16 h; protein lysates were then subjected to immu-noblotting using antibodies against PARP, caspase-3, caspase-7, cas-pase-8, caspase-9, or β-actin. FL, full length; CF, cleaved fragment. **c** MM.1S cells were treated with DMSO control or WL40 (200 nM) for 12 h, followed by measurement of caspase-3, caspase-8, or caspase-9 enzymatic activity (mean ± SD; $n = 3$; $p < 0.0001$). **d** MM.1S and ANBL6.BR cells were treated with DMSO control or WL40 (200 nM for MM.1S; 1 μM for ANBL6.BR) for 16 h; protein lysates were then subjected to immunoblotting using specific anti-bodies against cyclin-B1, CDC25C, CDC2, or β-actin. **e** ANBL6.BR cells were treated with DMSO control, WL40 (1 μM), or RA190 (1 μM) for indicated time periods; protein lysates were subjected to immunoblotting using specific antibodies against p53, p21, BIP, PERK, p-eIF2α, calnexin, LC3A/B, and β-actin. **f** MM.1S cells were treated with DMSO control, WL40 (200 nM), or RA190 (300 nM) for indicated time periods; protein lysates were subjected to immunoblotting using specific antibodies against p53, p21, BIP, PERK, p-eIF2α, calnexin, LC3A/B, and β-actin. Blots shown are representative of three independent experiments

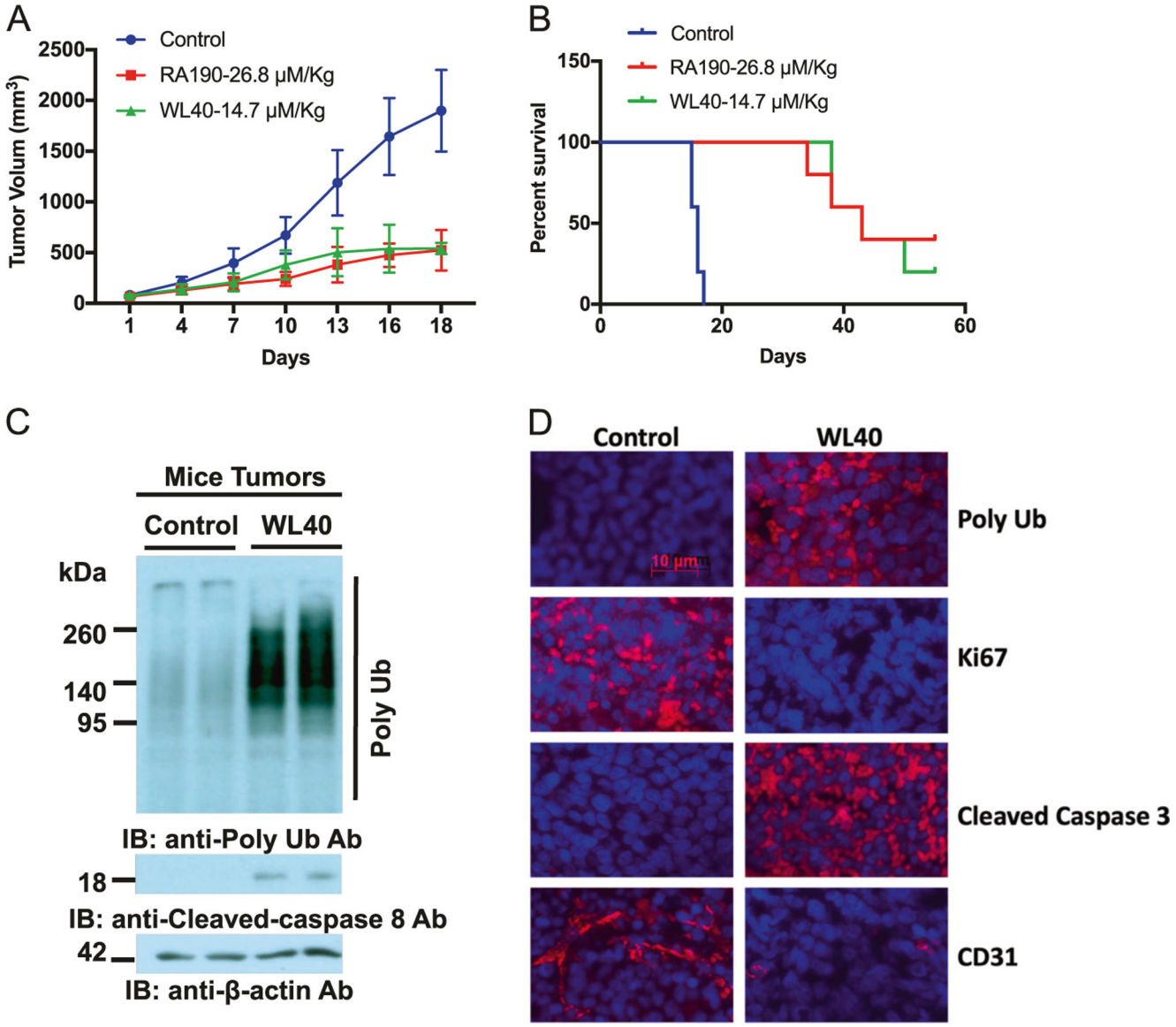

Fig. 5.

WL40 inhibits xenografted human MM cell growth and prolongs host survival. **a** Mice bearing human MM.1S MM tumors were treated with either vehicle control, WL40 (14.7 μM/kg; i. p.), or RA190 (26.8 μM/kg; i.p.) twice weekly for 18 days. Tumor volume (mean tumor volume ± SD in mm^3, 10 mice/ group) versus time is shown. **b** Kaplan–Meier plots shows survival of mice. **c** Lysates of tumors harvested from control-, WL40- and RA190-treated mice were subjected to immunoblot analysis using antipolyubiquitin, anticleaved-caspase-8, or anti-β-actin Abs. **d** Tumor sections from vehicle control-, and WL40-treated mice were stained with antipolyubiquitin, Ki67, caspase-3 (cleaved form), and CD31 Abs. Scale bar, 10 μm